

Accurate Decay Measurements of Nuclear Isotopes Embedded in Cryogenic Detectors

Spencer Fretwell
Colorado
School of Mines

Geon-Bo Kim
Lawrence Livermore
National Lab

Dongwon Lee
Lawrence Livermore
National Lab

Kyle Leach
Colorado
School of Mines

Stephan Friedrich
Lawrence Livermore
National Lab

ABSTRACT

The decay of radioactive isotopes can be characterized with high accuracy if they are embedded into detectors so that all decay products are captured and the total energy of each decay is measured with ~100% efficiency. This approach is especially promising when a cryogenic detector with high energy resolution is used that can separate signals from different isotopes or different decay channels. We are developing cryogenic detectors with operating temperatures of ~0.1 K for high-resolution measurements of nuclear decays. Here we present accurate decay measurements of Be-7 implanted into superconducting tunnel junction (STJ) detectors in the context of a search for hypothetical sterile neutrino particles. We also show safeguards-relevant work on magnetic microcalorimeter (MMC) detectors that can accurately measure isotope ratios of small actinide samples and identify contaminants. In both sensors, the experimental accuracy depends on the counting statistics of the measurement and on precise knowledge of the detector response function.

INTRODUCTION

The 2018 IAEA Research and Development Plan emphasizes the importance of "state-of-the-art tools, techniques, methodologies and expertise required for effective and efficient safeguards" [1]. R&D into advanced analytical instruments is critical in the current Programme for Nuclear Verification to support priority T.2 to "enhance sensitivity, reliability, and timeliness in sample analysis" [2]. Specifically, the current biennial Programme has identified the determination of plutonium isotopic mass ratios in very small samples by microcalorimetry as a late-term goal of priority SGAS-001 [2].

Cryogenic microcalorimeters with operating temperatures below 0.1 K and very high energy resolution may offer solutions to some of the current challenges in nuclear sensing. For example, small samples with low activity can be difficult to measure, as low statistics complicate the identification of certain isotopes and thus the verification of the sample composition. Microcalorimeters offer a solution by embedding samples into the active area of the device, providing 100% capture efficiency of decay event energy. This, combined with the inherently high energy resolution of low-temperature detectors, can provide good signal statistics required to accurately analyze small samples with low activity.

This paper describes two current developments for nuclear experiments with cryogenic detectors. The first is for accurate measurements of the decay of ^7Be embedded into superconducting tunnel junction (STJ) detectors. It is a fundamental physics experiment which utilizes STJ detectors to search for details in the recoil spectrum that would indicate the presence of a sterile neutrino admixture to the electron neutrino. The ^7Be decay is also relevant for the creation of ^7Li in the context of nuclear astrophysics, and we show that our spectral analysis techniques are applicable to safeguards research to extract isotope ratios and detection limits. The second part of this paper describes the development of magnetic microcalorimeters (MMCs) for accurate actinide analysis in nuclear safeguards. We show that MMCs can measure ^{244}Cm alpha spectra with an energy resolution of 4.5 keV at 5.8 MeV and identify isotopic impurities and decay products. This MMC performance is sufficient for follow-on experiments in which the actinide particles will be directly embedded into the detector for Pu assay of safeguards samples.

A Sterile Neutrino Search with Superconducting Tunnel Junctions

Superconducting tunnel junction (STJ) radiation detectors consist of two superconducting electrodes separated by thin insulating tunnel barrier (Figure 1). Energy from a nuclear decay in one of the electrodes breaks Cooper pairs and excites single electrons above the superconducting energy gap Δ . The resulting increase in tunneling current provides a direct measure of the deposited energy E , and the small $\sim\text{meV}$ superconducting energy gap enables a very high energy resolution E_{FWHM} of

$$E_{FWHM} = 2.355 \sqrt{\left(\varepsilon E \left(F + 1 + \frac{1}{\langle n \rangle} \right) \right)}. \quad (1)$$

Here $\varepsilon = 1.7\Delta$ is the average energy to generate an excited electron, $F = 0.2$ is the Fano factor for STJs, and $1+1/\langle n \rangle$ describes statistical fluctuations in the tunneling process. For an energy gap $\Delta_{\text{Ta}} = 0.7 \text{ meV}$, STJs can have an energy resolution of order $\sim 1 \text{ eV}$ at an energy $E = 100 \text{ eV}$ [3].

We are currently using STJ detectors to search for evidence of hypothetical dark matter particles called sterile neutrinos [4, 5]. For this, radioactive ^7Be is implanted into the STJ, which decays by electron capture into ^7Li and a neutrino. The neutrino escapes, and the STJs measure the $\sim 56 \text{ eV}$ recoil energy of the ^7Li daughter nucleus with a resolution of a few eV FWHM (Figures 2 – 4). Creation of a sterile neutrino with a mass in the keV range would reduce the recoil energy and create additional peaks in the spectrum. The experiment is nicknamed the *BeEST* for “*Be* Electron capture in Superconducting Tunnel junctions”.

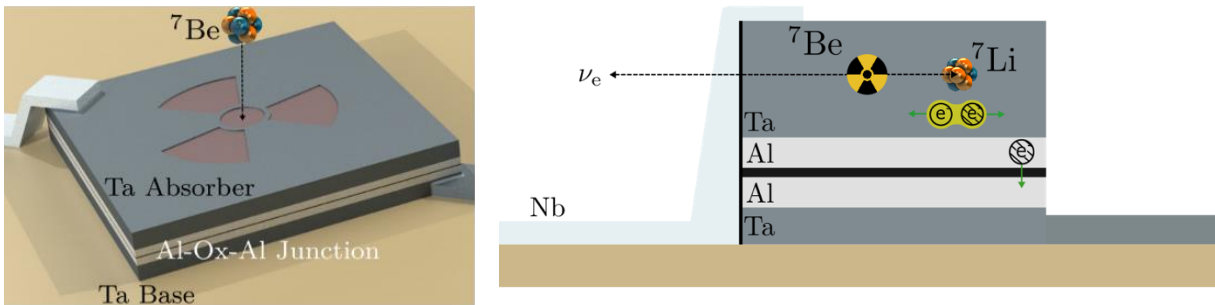


Figure 1 (left): Schematic of a Ta-Al-AlOx-Al-Ta STJ radiation detector with implanted ^7Be . Figure 2 (right): Upon decay of the ^7Be , the neutrino escapes from the STJ, and the recoiling ^7Li daughter breaks Cooper pairs and creates a tunnel current signal due to the increased number of excited electrons.

The observed recoil spectrum actually contains several peaks, because ${}^7\text{Be}$ can capture either a 1s electron (“K-capture”) or a 2s electron (“L-capture”), and in both cases the ${}^7\text{Li}$ can be produced in its ground state (GS) or in an excited state (ES). In addition, shake-up and shake-off effects produce a high-energy tail above all lines, and the escape of KLL Auger electrons produces a low-energy tail below the two K-capture peaks (Figure 3).

We can model the primary peaks with Gaussian functions and the tails with exponentially modified Gaussians and fit the observed spectrum accurately (Figure 3). One important number to extract from this spectrum is the ratio of L-capture and K-capture events, because it affects models of ${}^7\text{Li}$ production in nuclear astrophysics [4]. The best fit to the data uses a sum of 3 Gaussian functions for each peak and extracts an L/K capture ratio of 0.07165 with a statistical uncertainty of ± 0.00029 and reduced $\chi^2 = 0.95$. This sum of multiple Gaussians is required to accurately model the shapes of the peaks, which are broadened by chemical shifts beyond the STJ detector resolution. However, it is not obvious that there should be exactly three Gaussians, or even whether Gaussians are the correct functions to model the peaks with. In addition, it is not known whether the shake-up tails of the L-capture peaks are as strong as the tails of the K-capture peaks, or whether the peak/tail ratio can be allowed to vary in the fits. We have therefore systematically varied the number and type of fit functions over a range of plausible alternatives. The different fits produce L/K ratios between 0.064 and 0.078 with reduced χ^2 values between 0.95 and 1.41. This range is dominated by the uncertainty of the fit in the region from 60 to 70 eV and reflects L/K ratios that are consistent with the data for a variety of assumptions in the underlying physics. Taking into account these differences, we determine a value of $L/K = 0.0702(66)_{\text{sys}}(3)_{\text{stat}}$ [4].

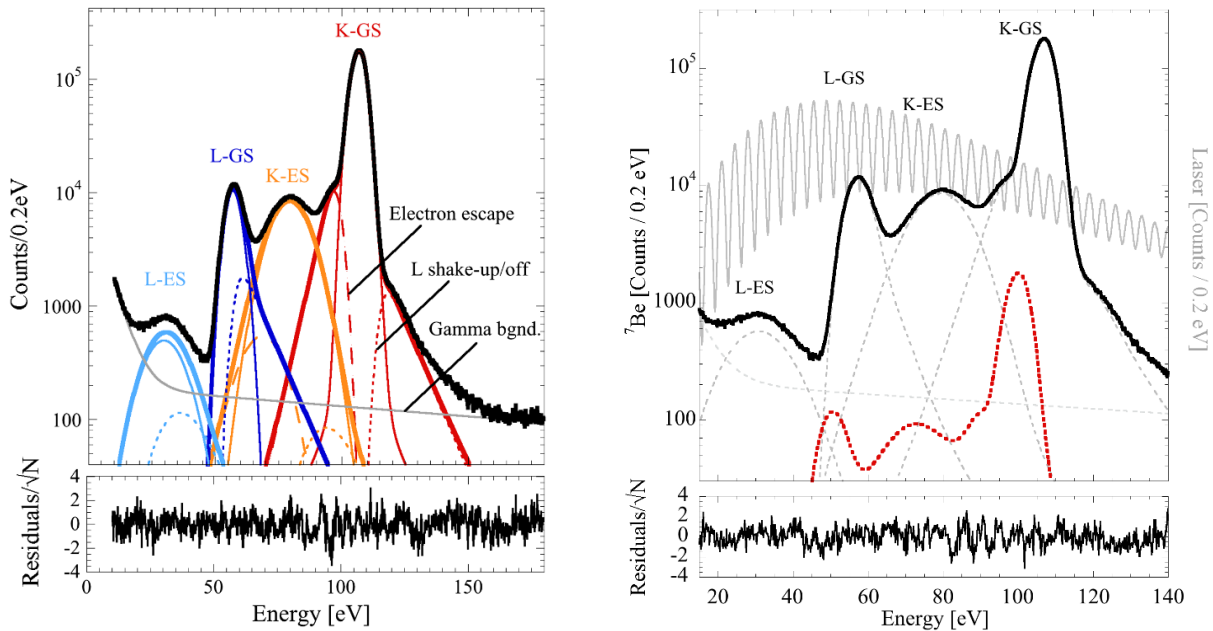


Figure 3 (left): The decay spectrum of ${}^7\text{Be}$ implanted into STJ detectors shows the four peaks due to K- and L-capture into the ground and excited state of ${}^7\text{Li}$, respectively. Tails due to shake-up and shake-off effects and electron escape must be taken into account to accurately fit the spectrum (from [4]). Figure 4 (right): The same spectrum can be used to look for evidence of hypothetical sterile neutrino dark matter. As an example, the red spectrum is the simulated signal if sterile neutrinos with a mass of 300 keV that were produced in 1% of the decays. The gray pulsed laser spectrum is used for accurate energy calibration (from [5]).

This measurement is an illustrative example for the importance of high energy resolution and an accurate understanding of the detector response function, because uncertainties in the response function can degrade the accuracy of a line ratio measurements well beyond the statistical limit. Similar effects often dominate isotope ratio measurements from alpha spectroscopy in nuclear safeguards and reinforce the need for improved detector technology for accurate Pu isotope assays.

However, the primary purpose of the *BeEST* experiment is to look for evidence of sterile neutrinos in the decay of ${}^7\text{Be}$. For this, the challenge is to detect weak peaks in the spectrum due to sterile neutrinos on top of a large background due to decays with (active) electron neutrinos (Figure 4). This task is similar to detecting the weak signals from minor isotopes and impurities in alpha spectra from safeguards samples or excluding the presence of certain isotopes. In a simplified analysis, the detection limit is given by the number of atoms in a sample that would produce a signature at the characteristic energy of the isotope that exceeds the background noise by at least a factor of 5. More accurately, we calculate the limit by assuming that the fit curve in Figure 4 describes the null hypothesis of a ${}^7\text{Be}$ decay involving only active neutrinos and represents the background in our search. We then generate a heavy neutrino spectrum for a certain mass by shifting the recoil peaks according to the calculated reduction in ${}^7\text{Li}$ recoil energy and scaling the amplitudes of the background spectrum by the probability of sterile neutrino creation. As an example, the measured ${}^7\text{Be}$ spectrum and a hypothetical signal from a sterile 300 keV neutrino that is produced in 1% of all decays are shown in Figure 4. The signal amplitude is then varied systematically for a given sterile neutrino mass, and maximum likelihood values is obtained for each signal amplitude by varying the amplitude and the peak centroids of the background. We numerically construct a Bayesian posterior function from this profiled likelihood and a flat prior for positive signal amplitudes, and extract 95% upper limits for sterile neutrino generation of order 10^{-4} from it [5]. These measurements currently provide the most stringent limits on the existence of sterile neutrinos in the mass range between 100 and 850 keV. The procedure used to extract these limits is also an example of how to calculate detection limits for minor isotopes in safeguards samples.

Actinide Measurements for Nuclear Safeguards

Magnetic microcalorimeters (MMCs) consists of a radiation absorber and a paramagnetic sensor at temperatures <0.05 K in a small magnetic field so that the Zeman levels are split and unevenly occupied. Particles from a nuclear decay heat both the absorber and the magnetic sensor in proportion to the absorbed energy and excite the spins of the sensor into the higher-energy state, and the resulting change in magnetization is read out with a SQUID preamplifier (Figure 5, 6).

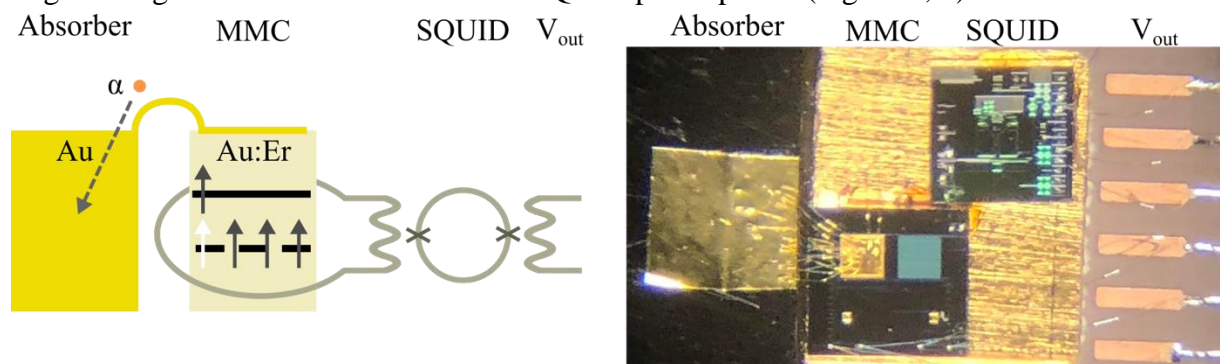


Figure 5 (left): Schematic of an MMC for alpha detection. Figure 6 (right): Picture of the MMC used in this experiment

Like all microcalorimeters, MMCs have a limiting energy resolution of

$$E_{FWHM} = 2.355\xi\sqrt{k_B T^2 C} \quad (1)$$

Here T is the operating temperature and C the heat capacity of the detector, and ξ is a factor of order unity that depends on the specific detector design. Equation (2) illustrates that high energy resolution requires low operating temperatures and small absorber dimensions for low heat capacity C . It can be understood by considering that MMC temperature measurements are microscopically based on measuring phonons with an average energy of $\sim k_B T$. If a detector at temperature T has a heat capacity C , it contains a total energy of CT corresponding to an average number of $CT/k_B T \approx C/k_B$ phonons. Thermal fluctuations between the detector and the cold bath of the refrigerator will cause this number to fluctuate by $\sqrt{C/k_B}$. Because each of these phonons carries an average energy of $\sim k_B T$, the energy measurements will fluctuate by $k_B T \sqrt{C/k_B} = \sqrt{k_B T^2 C}$. Equation (2) is analogous to the familiar expression of the energy resolution for semiconductor and STJ detectors where $E_{FWHM} = 2.355\sqrt{F\varepsilon E}$, if the energy ε to generate a single signal carrier is replaced by the average phonon energy $k_B T$, the energy E of the radiation is replaced by the total thermal energy CT of the sensor (which exceeds the energy of the radiation significantly), and the Fano factor F is replaced by ξ^2 .

We are developing MMCs with gold absorbers and erbium-doped silver (Ag:Er) and gold (Au:Er) sensors for actinide analysis in nuclear safeguards (Figure 6) [6-8]. The absorbers consist of gold foils up to 50 μm thick for 100% absorption efficiency for alpha particles. The goal of the project is to fully enclose the actinide sample in the Au absorber foil and combine 100% absorption efficiency with a high energy resolution to fully separate decay signals of interest. Here we present initial experiments to characterize the MMCs with an external ^{244}Cm alpha source and demonstrate their high energy resolution in the energy range of interest.

The MMC for this experiment uses a Au:Er sensor with a thin Au layer on top for uniform thermalization [9]. A 25 μm thick Au absorber foil is bonded to the thermalization layer with several Au bond wires so that the entire MMC is metallic and has a high thermal conductivity and (relatively) fast rise times (Figure 6). The absorber is exposed to a commercial 0.1 μCi ^{244}Cm source at a distance of 3.2 mm through a 1 mm diameter collimator at a temperature of 35 mK for a count rate of 5.4 counts/s. The source had last been chemically purified on 10/24/2011, after which time the ^{240}Pu daughter has slowly grown in. Its Cm isotopes were measured by the supplier by mass spectrometry on 10/19/2018, except for ^{243}Cm , which was measured by alpha spectroscopy due to the presence of ^{243}Am impurities. Since then, the isotopes have decayed over a period of 1.8 years until the measurement was started on 08/06/2020. The source composition is summarized in Table 1.

We have performed Geant-4 simulations of the expected alpha spectrum to estimate the high-energy tails of alpha peaks from decays into excited states of the daughter nuclei (Figure 7). For these decays, electrons emitted in the subsequent relaxation of the daughter can be absorbed in coincidence with the alpha particle, add their energy to the alpha energies and create high-energy tails at the corresponding peaks. For our source, this effect only matters for the strong ^{244}Cm alpha peak at 5763 keV. Other peaks in the spectrum are too weak, and the ^{244}Cm decay to the ^{240}Pu ground state is not accompanied by additional relaxation electrons.

Table 1. Source Composition

Nuclide	Half-Life [years]	Known Activity % (10/19/2018)	Expected Activity % (08/06/2020)	Measured Activity % (08/06/2020)
Cm-243	28.9(4)	0.01282	0.01315	0.015(6)
Cm-244	18.11(3)	99.8563	99.8269	99.773(8)
Cm-245	8423(74)	0.0111	0.0119	0.009(2)
Cm-246	4706(40)	0.1070	0.1146	0.078(3)
Cm-247	1.56(5)e7	0.0000	0	Not detected
Cm-248	3.48(6)e5	0.00001	0.00001	Not detected
Am-243	7364(22)	0.01292	0.0138	0.014(1)
Pu-240	6561(7)	0 as of 10/24/2011	0.1105	0.111(3)

The alpha-induced pulse traces were captured with a 14-bit ADC and written to disc for off-line analysis. The signals were processed with a trapezoidal filter with 0.7 ms peaking time and 0.3 ms gap time and corrected for drift and pile-up. The resulting spectrum has an energy resolution of 5.5 keV FWHM at 5.8 MeV, broadened beyond the detector resolution of 4.4 keV by energy loss of the alpha particles in the source (Figure 8). This is significantly better than the resolution of Si-based alpha detectors [10] and is one of the reasons why microcalorimeters are interesting for Pu analysis, since it allows separating ^{239}Pu and ^{240}Pu signals that overlap in conventional alpha spectra.

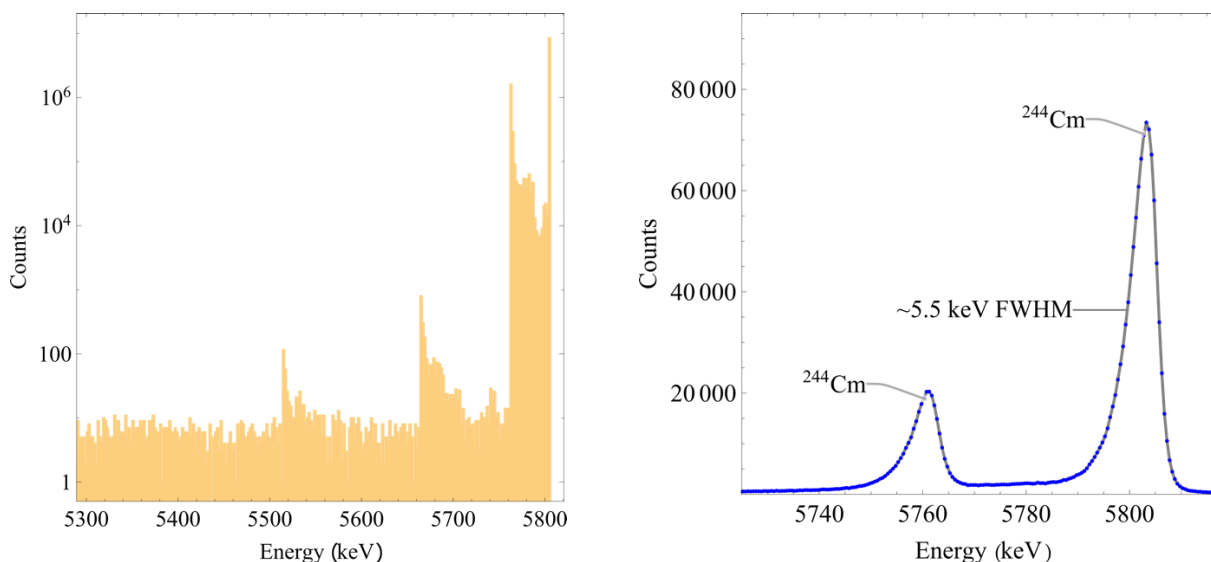


Figure 7 (left): A Geant-4 simulation of the ^{244}Cm spectrum shows the high-energy tails above alpha peaks from the decay into excited states of ^{240}Pu . They are caused by the coincident absorption of electrons from the relaxation of the ^{240}Pu daughter nucleus to its ground state. The structure in the tails is due to the specific energy levels in ^{240}Pu . **Figure 8 (right):** The two primary ^{244}Cm alpha peaks can be measured with an energy resolution of 4.4 eV FWHM. The MMC contributes 4.1 keV to this broadening, and the remainder is due to alpha energy loss in the source.

The full spectrum was then fit using a response function extracted from the two primary ^{244}Cm peaks (Figure 9). It consists of a Gaussian for the peak and three exponentially modified Gaussian (EMG) functions for the tail [10]:

$$EMG(A, \mu, \sigma, \tau, x) = \frac{A}{2|\tau|} e^{\frac{\mu-x}{\tau} + \frac{\sigma^2}{2\tau^2}} \operatorname{erfc}\left(\frac{\tau\left(\mu + \frac{\sigma^2}{\tau} - x\right)}{\sqrt{2}\sigma|\tau|}\right) \quad (3)$$

Here A , μ and σ are the usual Gaussian amplitude, mean and rms width, τ is the decay scale of the tail and erfc is the complementary error function. All fit functions share the same width $\sigma = \text{FWHM}/2.355$ that is set by the MMC detector resolution. Adding a fourth tail to the response function would improve the fit for energies below 5200 keV.

The spectrum shows the presence of ^{245}Cm , ^{246}Cm and ^{243}Am impurities, as well as the ^{244}Cm daughter ^{240}Pu . The two strong ^{244}Cm lines have a measured ratio of 0.3004(11), in agreement with the literature value of 0.3004(14). This uncertainty of 0.37% is dominated by the fit accuracy of the response in the region between the two strong peaks with the coincident electron signals, since the statistical contribution to the uncertainty is only 0.18%. The measured $^{246}\text{Cm}/^{244}\text{Cm}$ activity ratio of 0.078(3) is lower than expected and we are currently investigating possible causes. The weak signal from ^{245}Cm at 5361 keV contains only ~ 140 counts and is just at the detection limit. Its measured activity of 0.009(2)% is slightly lower than (although still within 2σ of) the expected value of 0.012%, possibly because the background approximation does not accurately extend to lower energies, which particularly affects weak lines. While the strong ^{244}Cm signals obscure the ^{243}Cm lines at 5785 and 5742 keV, the weak ^{243}Cm lines at 5992, 6058 and 6066 keV fall in a region of negligibly small spectral background and produce a measurable total of 29 counts. The ^{247}Cm and ^{248}Cm concentrations are below the detection limit. The measured $^{240}\text{Pu}/^{244}\text{Cm}$ ratio implies a source age of 8.9 ± 0.25 years since the last chemical separation. This agrees with the known age of 8.8 years. Similarly, the ^{243}Am concentration agrees with the source specifications. The measured activities are summarized in Table 1.

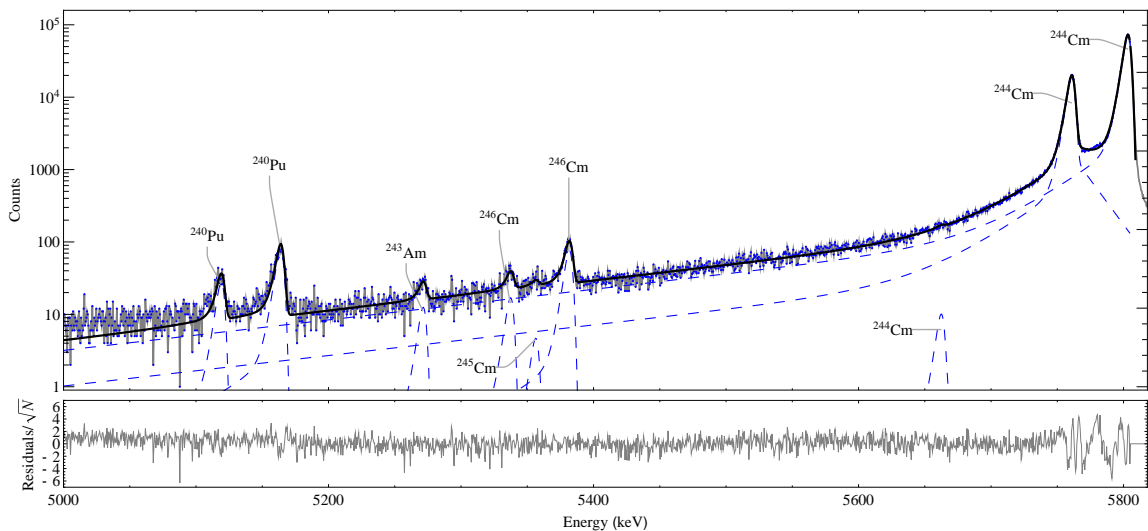


Figure 9. The full MMC alpha spectrum shows the signals from Cm and ^{243}Am impurities and the daughter nucleus ^{240}Pu . The electron coincidence tail causes systematic uncertainties in the fit at high energies.

The high energy resolution of 4.4 keV FWHM at 5.8 MeV demonstrates the potential for alpha and/or decay energy spectroscopy with MMCs. At the same time, the tails due to energy loss in the source and coincident electron absorption limit the accuracy of the measured line ratios. For this reason, we are currently developing techniques to enclose the source in the absorber such that the full energy of the decay is recorded and the tails are greatly reduced, in the ideal case close to zero [11].

CONCLUSIONS

Nuclear decays can be characterized with 100% efficiency if the radioisotope is embedded inside the detector. If cryogenic detectors with operating temperatures around 0.1 K are used for these measurements, their ultra-high energy resolution allows separating signals from different isotopes or decay channels. This approach can be used with ^7Be implanted into superconducting tunnel junction (STJ) detectors to perform a highly sensitive search for sterile neutrino dark matter. We are now also developing magnetic microcalorimeter (MMC) to use this approach in nuclear safeguards to assay small actinide particles embedded into their Au absorbers. In initial characterization experiments with an external ^{244}Cm alpha source, our MMCs have shown an energy resolution of 4.4 keV at 5.8 MeV. This exceeds the limits of Si alpha detector performance and is sufficient to separate most actinide signals of interest, including ^{239}Pu and ^{240}Pu . So far, the accuracy of the assay is often still limited by uncertainties in the detector response function. We have therefore started to develop techniques to integrate the actinide source into the Au absorber of our MMCs so that the response function will be greatly simplified.

ACKNOWLEDGEMENTS

This research was performed under appointment to the Nuclear Nonproliferation International Safeguards Fellowship Program sponsored by the Department of Energy, National Nuclear Security Administration Office of International Nuclear Safeguards (NA-241). It was performed under the auspices of the U.S. Department of Energy by Lawrence Livermore National Laboratory under Contract No. DE-AC52-07NA27344. (LLNL-PROC-825416)

REFERENCES

- [1] IAEA Safeguards Research and Development Plan, No. STR-385 (2018)
- [2] IAEA Development and Implementation Support Programme for Nuclear Verification 2020 - 2021, No. STR-393 (2020)
- [3] M. Kurakado, "Possibility of High-resolution Detectors using Superconducting Tunnel Junctions", *Nucl. Inst. Meth. A* **196**, 275 (1982).
- [4] S. Fretwell, K. G. Leach, C. Bray, G. B. Kim, J. Dilling, A. Lennarz, X. Mougeot, F. Ponce, C. Ruiz, J. Stackhouse, S. Friedrich, "Direct Measurement of the ^7Be L/K Capture Ratio in Ta-Based Superconducting Tunnel Junctions", *Phys. Rev. Lett.* **125**, 032701 (2020)
- [5] S. Friedrich, G. B. Kim, C. Bray, R. Cantor, J. Dilling, S. Fretwell, J. A. Hall, A. Lennarz, V. Lordi, P. Machule, D. McKeen, X. Mougeot, F. Ponce, C. Ruiz, A. Samanta, W. K. Warburton, K. G. Leach, "Limits on the Existence of sub-MeV Sterile Neutrinos from the Decay of ^7Be in Superconducting Quantum Sensors", *Phys. Rev. Lett.* **126**, 021803 (2021)
- [6] C. R. Bates, C. Pies, S. Kempf, D. Hengstler, A. Fleischmann, L. Gastaldo, C. Enss, S. Friedrich, "Reproducibility and Calibration of MMC-Based High-Resolution Gamma Detectors", *Appl. Phys. Lett.* **109**, 023513 (2016)

**Proceedings of the INMM & ESARDA Joint Virtual Annual Meeting
August 23-26 & August 30-September 1, 2021**

- [7] G.-B. Kim, R. Hummatov, S. Kempf, C. Flynn, R. Cantor, A. Fleischmann, S. T. P. Boyd, C. Enss, S. Friedrich, "Consistent measurements of ^{233}U gamma emissions using metallic magnetic calorimeters with ultra-high energy resolution", *J. Radioanal. Nucl. Chem.* **318**, 803-808 (2018)
- [8] S. Friedrich, G.-B. Kim, R. Hummatov, T. Parsons-Davis, R. Cantor, "Magnetic Microcalorimeter Gamma-Detectors for High-Accuracy Nuclear Decay Data, *Proc. INMM* **51** (2018)
- [9] W. S. Yoon, G.-B. Kim, H. J. Lee, J. Y. Lee, J. H. Lee, Y. S. Jang, S. J. Lee, M. K. Lee, Y. H. Kim, "Fabrication of Metallic Magnetic Calorimeter for Radionuclide Analysis", *J. Low Temp. Phys.* **176**, 644 (2014)
- [10] F. Dayras, "Analysis of ^{239}Pu , ^{244}Cm and ^{243}Am alpha spectra using the unfolding code Colégram without prior use of a nuclear data library", *Nucl. Inst. Meth. A* **490**, 492 (2002)
- [11] A. S. Hoover, E. M. Bond, M. P. Croce, T. G. Holesinger, G. J. Kunde, M. W. Rabin et al. "Measurement of the $^{240}\text{Pu}/^{239}\text{Pu}$ Mass Ratio Using a Transition-Edge-Sensor Microcalorimeter for Total Decay Energy Spectroscopy", *Anal. Chem.* **87**, 3996 (2015)